




Roper-like resonances with various flavor contents and their two-pion emission decays

A. J. Arifi ¹, H. Nagahiro ^{1,2}, A. Hosaka ^{1,3} and K. Tanida ³

¹Research Center for Nuclear Physics (RCNP), Osaka University, Ibaraki, Osaka 567-0047, Japan

²Department of Physics, Nara Women's University, Nara 630-8506, Japan

³Advanced Science Research Center, Japan Atomic Energy Agency, Tokai, Ibaraki 319-1195, Japan



(Received 17 April 2020; accepted 28 May 2020; published 16 June 2020)

We study the three-body decay of the newly observed bottom baryon $\Lambda_b^*(6072)$ by LHCb; $\Lambda_b^*(6072) \rightarrow \Lambda_b \pi \pi$. Its mass about 500 MeV above the ground state Λ_b and a broad width imply that the state could be an analogue of the Roper resonance of the nucleon $N(1440)$. In terms of sequential processes going through Σ_b and Σ_b^* , we find that the observed invariant mass distribution is reproduced assuming its spin and parity $J^P = 1/2^+$. We discuss that the ratio of the two sequential processes and angular correlation of two pions are useful for the determination of spin and parity. We suggest further studies for the Roper resonance analogue in various flavor contents, raising an interesting and important question in baryon spectroscopy.

DOI: 10.1103/PhysRevD.101.111502

In this work, motivated by the recent observation of $\Lambda_b^*(6072)$ by CMS and LHCb collaborations [1,2], with the mass and width $M = 6072.3$ MeV and $\Gamma = 72$ MeV measured by LHCb [2], we discuss it as a state analogous to the Roper resonance $N(1440)$ with spin and parity $J^P = 1/2^+$ in heavy flavor sectors. It is shown that the three-body decay of two pion emission is particularly useful to determine its unknown spin and parity.

The Roper resonance is the first excited state of the nucleon of $J^P = 1/2^+$ [3]. It has been a mysterious state because its properties such as the mass and level ordering with negative parity nucleons have not been easily explained by the conventional quark model (for a recent review see for instance [4]). Detailed studies by a dynamical model for meson-baryon scatterings [5,6] and by the measurement of the transition form factor in a wide range of momentum transfer Q^2 [7] have convinced us that it is a radial excitation of the nucleon. Furthermore, several lattice simulations support this picture [8–10]. As demonstrated in [5,6], one promising physical interpretation is that the Roper resonance is a quark core coupled by meson clouds. The quark-meson interaction then has a significant effect in reducing the large mass of the quark core excitation. An alternative description was made in Ref. [11] where the pion (in general Nambu-Goldstone boson) exchange interaction reduced the mass of the quark core excitation. In this

way, the mass ordering of positive and negative parity baryons were well reproduced for nonstrange and strange baryons.

On the other hand, similar states of $J^P = 1/2^+$ with almost the same excitation energies have been known for some time for hyperons systematically [12,13]. The recent observation of $\Lambda_b^*(6072)$ could add another candidate in the list of the analogous states. In fact, there is also a candidate in the charm sector, $\Lambda_c^*(2765)$. Note that in PDG it is not yet determined whether it is Λ_c^* or Σ_c^* , but recent report suggests that it is likely to be an isoscalar Λ_c^* [14]. However, the spin and parity of these charmed and bottom candidates are not yet determined. Observing this situation, we show possible candidate states in Fig. 1 with their excitation energies. They are similar not only in masses but also in decays through two pion emission which is dominated by the sequential processes going through intermediate baryon resonances as shown in Fig. 2, while a nonresonant contribution is insignificant. These rather universal features in various flavor sectors may suggest important dynamics of low energy QCD.

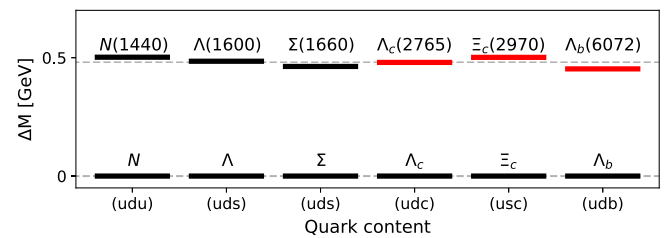


FIG. 1. Excitation energies of the first excited $J^P = 1/2^+$ baryons and candidates with various flavor contents. Red bars are for those with undetermined spin and parity.

Published by the American Physical Society under the terms of the Creative Commons Attribution 4.0 International license. Further distribution of this work must maintain attribution to the author(s) and the published article's title, journal citation, and DOI. Funded by SCOAP³.

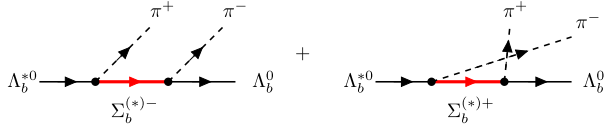


FIG. 2. Sequential decay processes of $\Lambda_b^{*0} \rightarrow \Lambda_b^0 \pi^+ \pi^-$ going through $\Sigma_b^{(*)-}$ and $\Sigma_b^{(*)+}$.

In the present work, focusing on $\Lambda_b^*(6072)$, we study in detail its three-body decay $\Lambda_b^*(6072) \rightarrow \Lambda_b^0 \pi \pi$. In our previous preprint [15], we have shown that the Dalitz plot analysis is particularly useful for the determination of spin and parity of $\Lambda_c^*(2765)$ when the decay is dominated by sequential processes going through Σ_c and Σ_c^* . The relevant diagrams are shown in Fig. 2 (for charmed baryons, replace the label b for bottom by c). Following this, we investigate the sequential decays of $\Lambda_b^*(6072)$ with an intermediate state Σ_b or Σ_b^* . In principle there are other processes that may contribute. They are for instance, a direct process where two pions are emitted at once at a single vertex, and a meson resonance process such as a scalar σ meson to which two pions couple. However, qualitative arguments are given for the reason that these processes may be suppressed for an analogous decay of $\Lambda_c^*(2765)$ [15]. Therefore, in this paper we will consider exclusively the sequential process, which can indeed explain the so far observed data very well as we will see later.

To compute these diagrams, let us first introduce amplitudes for various vertices. Because the bottom baryons are sufficiently heavy, we employ a nonrelativistic method. Assuming that the spin and parity of Λ_b^* equal $1/2^+$, the amplitudes at the first vertex of Fig. 2 are given by

$$\begin{aligned} -i\mathcal{T}_{\Lambda_b^* \rightarrow \Sigma_b \pi} &= g_1 \chi_{\Sigma_b}^\dagger (\boldsymbol{\sigma} \cdot \mathbf{p}) \chi_{\Lambda_b^*}, \\ -i\mathcal{T}_{\Lambda_b^* \rightarrow \Sigma_b^* \pi} &= g_2 \chi_{\Sigma_b^*}^\dagger (\mathbf{S}^\dagger \cdot \mathbf{p}) \chi_{\Lambda_b^*}, \end{aligned} \quad (1)$$

and for the second vertex,

$$\begin{aligned} -i\mathcal{T}_{\Sigma_b \rightarrow \Lambda_b \pi} &= g_3 \chi_{\Lambda_b}^\dagger (\boldsymbol{\sigma} \cdot \mathbf{p}) \chi_{\Sigma_b}, \\ -i\mathcal{T}_{\Sigma_b^* \rightarrow \Lambda_b \pi} &= g_4 \chi_{\Lambda_b}^\dagger (\mathbf{S} \cdot \mathbf{p}) \chi_{\Sigma_b^*}. \end{aligned} \quad (2)$$

In Eqs. (1) and (2), g_i 's are the coupling constants and χ 's are the two-component spinors for the baryons as indicated by lower indices. Moreover, we define the spin operator $\boldsymbol{\sigma}$ for spin-1/2 particle and the spin transition operator \mathbf{S} for transition from spin 3/2 to 1/2. The pion momentum for each vertex is denoted as \mathbf{p} .

By using these vertex amplitudes, the amplitude of the first diagram of Fig. 2 with the intermediate Σ_b^- is expressed as

$$-i\mathcal{T}[\Sigma_b^-] = -i \frac{\mathcal{T}_{\Sigma_b^- \rightarrow \Lambda_b^0 \pi^-} \mathcal{T}_{\Lambda_b^{*0} \rightarrow \Sigma_b^- \pi^+}}{m_{23} - m_{\Sigma_b^-} + \frac{i}{2} \Gamma_{\Sigma_b^-}}, \quad (3)$$

where m_{23} is the invariant mass of the subsystem π^- (particle 2) and Λ_b^0 (particle 3). The amplitudes with the Σ_b^+ intermediate state and those with $\Sigma_b^{*\mp}$ are computed similarly. The total amplitude is then the coherent sum of the four of them.

The unknown coupling constants g_i 's are constrained by the heavy quark spin symmetry of QCD [16]; the ratios of g_1 to g_2 and of g_3 to g_4 are computed when Σ_b and Σ_b^* are regarded as heavy quark spin partners. In the heavy quark limit, the spin J of a baryon is composed of a spin j of the brown muck of light degrees of freedom [17] and spin 1/2 of the heavy quark, such that $J = j \pm 1/2$.

For a spin 1/2 Λ_b^* , the brown muck spin can take two values, $j = 0, 1$. Assume further that the brown muck of $\Sigma_b^{(*)}$ has spin $j = 1$ as in the quark model, their total spin J can be 1/2 or 3/2. Having this information, we can compute the ratio as [15,18]

$$\frac{g_2}{g_1} = \sqrt{2} \quad \text{for } j = 0 \quad \text{and} \quad \frac{1}{\sqrt{2}} \quad \text{for } j = 1 \quad (4)$$

for Λ_b^* with $J^P = 1/2^+$. Combined with two-body phase space factors, when the same partial L -wave is possible for the two final states $\pi \Sigma_b$ and $\pi \Sigma_b^*$, we find the ratio

$$R = \frac{\Gamma(\Lambda_b^*(6072) \rightarrow \Sigma_b^* \pi)}{\Gamma(\Lambda_b^*(6072) \rightarrow \Sigma_b \pi)} = \frac{g_2^2 p_2^{2L+1}}{g_1^2 p_1^{2L+1}} \quad (5)$$

where the ratio of g_2/g_1 is constrained by the heavy quark spin symmetry as in Eq. (4).

For $J^P = 1/2^+$, the two decays are in p -wave, $L = 1$. Using $p_1 = 215$ MeV and $p_2 = 192$ MeV, we obtain

$$R = 1.43 \quad \text{for } j = 0 \quad \text{and} \quad 0.36 \quad \text{for } j = 1 \quad (6)$$

As we will see shortly, this agrees well with the observed data from LHCb. On the other hand, if $J^P = 1/2^-$ the partial waves of $\pi \Sigma_b$ and of $\pi \Sigma_b^*$ are s and d -waves, respectively. For low momentum pion as in the present case, the d -wave decay is suppressed as compared to the s -wave decay. Therefore, we find $R \ll 1$ which does not seem consistent with the experimental data. This demonstrates the advantage in the use of the ratio R for spin and parity.

Now we discuss Dalitz plots and other related quantities. In what follows, we assume again $J^P = 1/2^+$ for $\Lambda_b^*(6072)$. For decays of unpolarized particles, Dalitz plots are expressed as functions of two kinematical variables formed by the three decaying particles. In fact, they also depend on the mass of the initial particle, which distributes over a finite range of width ~ 72 MeV for $\Lambda_b^*(6072)$.

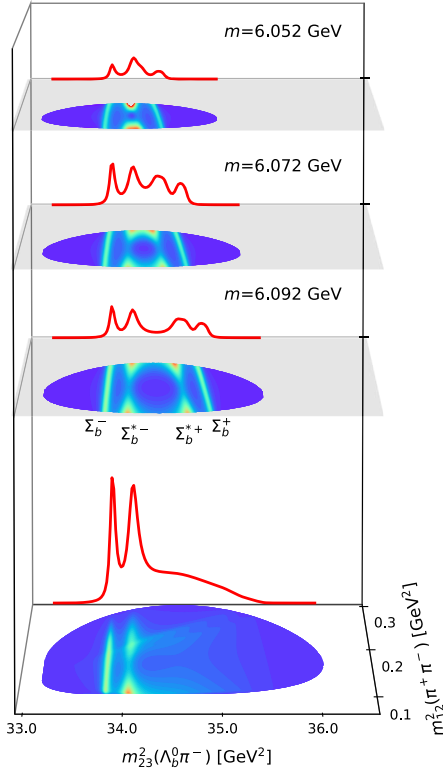


FIG. 3. The Dalitz and invariant mass plots at three different initial masses of $\Lambda_b^*(6072)$ (upper three panels) and the convoluted one (bottom panel).

In experiments with low statistics, plots are often made by integrating the signals from such a finite mass range. Therefore, to compare directly theory predictions with the actual data, this feature is properly treated.

In the upper three panels of Fig. 3 are shown diagonal views of the Dalitz plots for decay probabilities

$$P(m; m_{12}^2, m_{23}^2) = \frac{1}{(2\pi)^3} \frac{1}{32m^3} \int \overline{|T|^2} dm_{12}^2 dm_{23}^2 \quad (7)$$

at three different fixed masses of $\Lambda_b^*(6072)$ around the peak value, $m(\Lambda_b \pi \pi) = 6.052, 6.072$ and 6.092 GeV, as functions of invariant mass squares m_{12}^2 and m_{23}^2 . Note that the invariant mass m_{23} is for $\Lambda_b \pi^-$ that couples to $\Sigma_b^{(*)-}$, which will be relevant in the discussions below. In each layer, the solid red curve shown in the back face is the projected strength, namely the invariant mass plot. In all the three plots, we find four resonance bands corresponding to Σ_b^- , Σ_b^{*-} , Σ_b^{*+} , and Σ_b^+ from the left to right. The first two are for the first diagram of Fig. 2 showing the genuine resonance band, while the latter two correspond to the second one that are the so called kinematical reflection.

Now what we need is the sum of the plots like these three ones. More precisely, the convolution is performed over the finite mass range weighted by the Breit-Wigner function,

$$P(m_{12}^2, m_{23}^2) = \frac{1}{N} \int \frac{P(m; m_{12}^2, m_{23}^2) dm}{(m - M_{\Lambda_b^*})^2 + \Gamma_{\Lambda_b^*}^2/4}, \quad (8)$$

where the factor N is for normalization and m for the $\Lambda_b \pi \pi$ mass. The result is shown in the bottom panel of Fig. 3 as well as the invariant mass plot on the back face. As shown there, in the convoluted plot the peaks of kinematical reflections in the upper three panels are smeared out, while the real resonance peaks remain.

Because the experimental data is shown for the sum of signals of $\Lambda_b \pi^+$ and $\Lambda_b \pi^-$, we have shown in Fig. 4 the corresponding one of our calculation (red solid curve) compared with the experimental data. We note that the blue curve in Fig. 4 for the $\Lambda_b \pi^-$ invariant mass plot is the same as the red curve on the back face of the bottom panel in Fig. 3. Note that experimental resolution of around 1 MeV is not considered in the calculation. For theory side, we have also shown the strengths of $\Lambda_b \pi^-$ and $\Lambda_b \pi^+$ separately by blue and green solid curves, respectively. We find that our theory calculation agrees remarkably well with experimental data not only in overall shape of the peaks and background. The relative strengths of the peaks is determined by the ratio R , while the background shape is reproduced by the convoluted kinematical reflection. It is interesting to see that even such a detailed structure, the relative height of the two resonance peaks of Σ_b and Σ_b^* are well reproduced. This is achieved by taking the sum of the two charged states. If only $\Lambda_b \pi^-$ is included, the left peak is slightly higher than that of the right one as shown in the bottom panel of Fig. 3 and by the blue curve in Fig. 4. This analysis so far supports the spin and parity of $\Lambda_b^*(6072)$ is $1/2^+$, and their decay is dominated by the two pion emission of the sequential processes. This is one of the main conclusions of the present study. If there will be further high statistics data, it is interesting to compare the Dalitz plots at each different energies.

Let us further look at the angular correlation (dependence) along the resonance band. The angle is the one

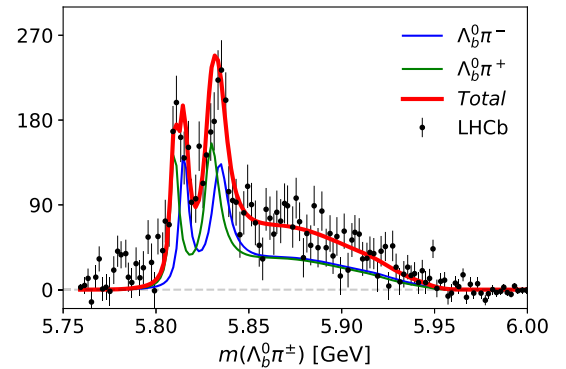


FIG. 4. Invariant mass plots of $\Lambda_b^0 \pi^-$ (blue), $\Lambda_b^0 \pi^+$ (green), and their sum (red). The data from LHCb is the sum of these two [2] and compared with the red curve.

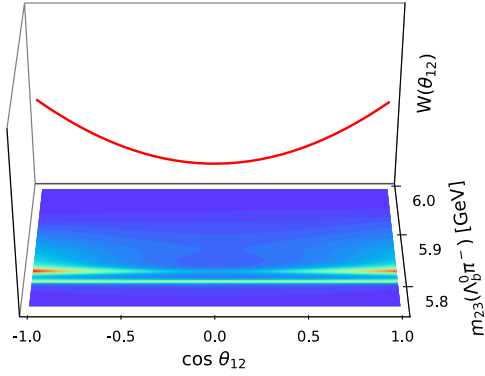


FIG. 5. The convoluted square Dalitz plot for $\Lambda_b^*(6072)$ and its corresponding angular correlation along Σ_b^{*-} with a mass cut $M_{\Sigma_b^{*-}} \pm \Gamma_{\Sigma_b^{*-}}$.

between the two pions θ_{12} in the intermediate resonance rest frame. To see the correlation better, it is convenient to make a square plot as a function of m_{23} and $\cos\theta_{12}$ as shown in the lower plot of Fig. 5. As seen there the angular correlation along the Σ_b band (near side) is flat due to its spin 1/2. On the other hand, the angular correlation along the Σ_b^* band (far side) has a concave shape due to its spin 3/2.

In general the angular correlation along the Σ_b^* band decaying from a particle of spin J contains the two terms weighted by the helicity amplitudes A_h , where h is the conserved helicity in the decay,

$$W(\theta_{12}) \propto |A_{1/2}(\Lambda_b^* \rightarrow \Sigma_b^* \pi)|^2 \times (1 + 3 \cos^2 \theta_{12}) + |A_{3/2}(\Lambda_b^* \rightarrow \Sigma_b^* \pi)|^2 \times 3 \sin^2 \theta_{12}. \quad (9)$$

When the initial Λ_b^* has spin 1/2, the helicity amplitude $A_{3/2}$ vanishes. Thus, the angular correlation will have a $1 + 3 \cos^2 \theta_{12}$ dependence (concave shape). In reality, interference between the resonance of a finite width and background (kinematical reflection in the present case) contaminates that angular correlation. Fitting the projected angular correlation as plotted in the upper panel of Fig. 3, our prediction for the angular correlation is

$$W(\theta_{12}) \propto 1 + 3.3 \cos^2 \theta_{12}. \quad (10)$$

So far we have focused our discussions on $\Lambda_b^*(6072)$. As anticipated in the beginning of this paper, there are other candidate baryons of similar nature, in particular Ξ baryons. One is $\Xi_c^*(2970)$ with excitation energy around 500 MeV and decays into $\Xi_c \pi \pi$ [19]. If it is regarded as a Roper-like resonance, its decay into $\Lambda_c K$ is forbidden due to the brown muck selection rule, namely the transition

of 0^+ (initial brown muck) $\rightarrow 0^+$ (final brown muck) $+ 0^-$ (kaon) does not occur. This selection rule applies to the other candidates and is a unique feature of the Roper like resonance.

In recent analysis, LHCb reported several resonances in $\Lambda_c K$ [20]. One of them is $\Xi_c^*(2965)$ with similar excitation energy, but it has significantly smaller decay width than $\Xi_c^*(2970)$. Therefore, $\Xi_c^*(2965)$ could be a particle of different nature that can be identified as a negative parity excitation of Ξ_c' as pointed out in Ref. [21,22]. Likewise, in the bottom sector, the $\Xi_b^*(6227)$ resonance observed in $\Lambda_b K$ and $\Xi_b \pi$ decays [23] would be this analogue of negative parity excitation of Ξ_b' [24–28]. We expect a Roper-like Ξ_b^* of $J^P = 1/2^+$ decaying into $\Xi_b \pi \pi$ at around 6.2 GeV.

We may expect further candidates in the strangeness sector. For example, the resonance $\Xi^*(1820)$ listed in PDG [12] may be identified with $3/2^-$ resonance as observed in ΛK invariant mass [29]. However, a resonance with a similar excitation energy is also observed in $\Xi \pi \pi$ invariant masses with a larger decay width [30]. This is a candidate of the Roper-like resonance.

Here we summarize several common features of the Roper-like resonances in our observation:

- (i) The excitation energy is around 500 MeV which is rather flavor-independent.
- (ii) The decay width is rather large with a significant coupling to two-pion emission decay.
- (iii) Their two-pion emission decays are dominated by the sequential processes going through $1/2^+$ resonance, e.g., Σ_b and $3/2^+$ resonance, e.g., Σ_b^* , or their analogues, indicating that the nonsequential contributions including those from $f_0(500)$ are insignificant as observed also for other baryons [31–33].
- (iv) The ratio R and angular correlation can be used to determine their spin and parity $1/2^+$.

Observations in the heavy flavor baryons and revisit to the light flavor baryons could provide new insights into unique flavor independent dynamics of low energy QCD.

We are thankful for support from the Reimei Research Promotion project (Japan Atomic Energy Agency) in completion of this work. A. J. A. is supported by a scholarship from the Ministry of Education, Culture, Science and Technology of Japan. H. N. is supported in part by Grants-in Aid for Scientific Research, Grants No. 17K05443(C) and A. H. by Grants No. 17K05441(C) and by Grants-in Aid for Scientific Research on Innovative Areas (No. 18H05407).

- [1] A. M. Sirunyan *et al.* (CMS Collaboration), Study of excited Λ_b^0 states decaying to $\Lambda_b^0\pi^+\pi^-$ in proton-proton collisions at $\sqrt{s} = 13$ TeV, *Phys. Lett. B* **803**, 135345 (2020).
- [2] R. Aaij *et al.* (LHCb Collaboration), Observation of a new baryon state in the $\Lambda_b^0\pi^+\pi^-$ mass spectrum, [arXiv:2002.05112](https://arxiv.org/abs/2002.05112).
- [3] L. D. Roper, Evidence for a P-11 Pion-Nucleon Resonance at 556 MeV, *Phys. Rev. Lett.* **12**, 340 (1964).
- [4] V. D. Burkert and C. D. Roberts, Colloquium: Roper resonance: Toward a solution to the fifty year puzzle, *Rev. Mod. Phys.* **91**, 011003 (2019).
- [5] N. Suzuki, B. Julia-Diaz, H. Kamano, T. S. H. Lee, A. Matsuyama, and T. Sato, Disentangling the Dynamical Origin of P-11 Nucleon Resonances, *Phys. Rev. Lett.* **104**, 042302 (2010).
- [6] H. Kamano, S. X. Nakamura, T. S. H. Lee, and T. Sato, Extraction of P11 resonances from πN data, *Phys. Rev. C* **81**, 065207 (2010).
- [7] I. Aznauryan *et al.* (CLAS Collaboration), Electroexcitation of nucleon resonances from CLAS data on single pion electroproduction, *Phys. Rev. C* **80**, 055203 (2009).
- [8] K. F. Liu, Baryons and chiral symmetry, *Int. J. Mod. Phys. E* **26**, 1740016 (2017).
- [9] J. J. Wu, D. B. Leinweber, Z. W. Liu, and A. W. Thomas, Structure of the Roper resonance from lattice QCD constraints, *Phys. Rev. D* **97**, 094509 (2018).
- [10] C. Lang, L. Leskovec, M. Padmanath, and S. Prelovsek, Pion-nucleon scattering in the Roper channel from lattice QCD, *Phys. Rev. D* **95**, 014510 (2017).
- [11] L. Glozman and D. Riska, The spectrum of the nucleons and the strange hyperons and chiral dynamics, *Phys. Rep.* **268**, 263 (1996).
- [12] M. Tanabashi *et al.* (Particle Data Group), Review of particle physics, *Phys. Rev. D* **98**, 030001 (2018) and 2019 update.
- [13] M. Takayama, H. Toki, and A. Hosaka, Systematics of the SU(3) baryon spectra and deformed oscillator quark model, *Prog. Theor. Phys.* **101**, 1271 (1999).
- [14] A. Abdesselam *et al.* (Belle Collaboration), Experimental determination of the isospin of $\Lambda_c(2765)^+/\Sigma_c(2765)^+$, [arXiv:1908.06235](https://arxiv.org/abs/1908.06235).
- [15] A. J. Arifi, H. Nagahiro, A. Hosaka, and K. Tanida, Three-body decay of $\Lambda_c^*(2765)$ and determination of its spin-parity, *Phys. Rev. D* **101**, 094023 (2020).
- [16] N. Isgur and M. B. Wise, Spectroscopy with Heavy Quark Symmetry, *Phys. Rev. Lett.* **66**, 1130 (1991).
- [17] M. Neubert, Heavy quark symmetry, *Phys. Rep.* **245**, 259 (1994).
- [18] H. Y. Cheng and C. K. Chua, Strong decays of charmed baryons in heavy hadron chiral perturbation theory, *Phys. Rev. D* **75**, 014006 (2007).
- [19] J. Yelton *et al.* (Belle Collaboration), Study of excited Ξ_c states decaying into Ξ_c^0 and Ξ_c^+ baryons, *Phys. Rev. D* **94**, 052011 (2016).
- [20] R. Aaij *et al.* (LHCb Collaboration), Observation of new Ξ_c^0 baryons decaying to $\Lambda_c^+K^-$, [arXiv:2003.13649](https://arxiv.org/abs/2003.13649).
- [21] H. Yang, H. Chen, and Q. Mao, Identifying the Ξ_c^0 baryons observed by LHCb as P -wave Ξ_c' baryons, [arXiv:2004.00531](https://arxiv.org/abs/2004.00531).
- [22] K. Wang, L. Xiao, and X. Zhong, Understanding the newly observed Ξ_c^0 states through their decays, [arXiv:2004.03221](https://arxiv.org/abs/2004.03221).
- [23] R. Aaij *et al.* (LHCb Collaboration), Observation of a New Ξ_b^- Resonance, *Phys. Rev. Lett.* **121**, 072002 (2018).
- [24] B. Chen, K. W. Wei, X. Liu, and A. Zhang, Role of newly discovered $\Xi_b(6227)^-$ for constructing excited bottom baryon family, *Phys. Rev. D* **98**, 031502(R) (2018).
- [25] E. L. Cui, H. M. Yang, H. X. Chen, and A. Hosaka, Identifying the $\Xi_b(6227)$ and $\Sigma_b(6097)$ as P -wave bottom baryons of $J^P = 3/2^-$, *Phys. Rev. D* **99**, 094021 (2019).
- [26] K. L. Wang, Q. F. Lu, and X. H. Zhong, Interpretation of the newly observed $\Sigma_b(6097)^\pm$ and $\Xi_b(6227)^-$ states as the P -wave bottom baryons, *Phys. Rev. D* **99**, 014011 (2019).
- [27] H. Yang, H. Chen, E. Cui, A. Hosaka, and Q. Mao, Decay properties of P -wave bottom baryons within light-cone sum rules, *Eur. Phys. J. C* **80**, 80 (2020).
- [28] D. Jia, W. N. Liu, and A. Hosaka, Regge behaviors in orbitally excited spectroscopy of charmed and bottom baryons, *Phys. Rev. D* **101**, 034016 (2020).
- [29] S. Biagi, M. Bourquin, R. Brown, H. Burekhart, P. Extermann, M. Gaillard, C. P. Gee, W. Gibson, P. Jacot-Guillarmod, J. Perrier, K. Ragan, P. Rosselet, P. Schirato, H. Siebert, V. Smith, K. Streit, J. Thresher, A. Wood, and C. Yanagisawa, Ξ^* resonances in Ξ^- Be interactions. 2. Properties of $\Xi(1820)$ and $\Xi(1960)$ in the $\Lambda\bar{K}^0$ and $\Sigma^0\bar{K}^0$ channels, *Z. Phys. C* **34**, 175 (1987).
- [30] S. Apsell *et al.*, Evidence for Ξ Resonances in the $\Xi(1530)\pi$ System, *Phys. Rev. Lett.* **24**, 777 (1970).
- [31] S. Prakhov *et al.* (Crystal Ball Collaboration), Measurement of $\pi^-p \rightarrow \pi^0\pi^0n$ from threshold to $p(\pi^-)$ 750-MeV/ c , *Phys. Rev. C* **69**, 045202 (2004).
- [32] S. Prakhov *et al.* (Crystal Ball Collaboration), Reaction $K^-p \rightarrow \pi^0\pi^0\Lambda$ from $p_{K^-} = 514$ -MeV/ c to 750-MeV/ c , *Phys. Rev. C* **69**, 042202(R) (2004).
- [33] R. Mizuk *et al.* (Belle Collaboration), Experimental Constraints on the Possible J^P Quantum Numbers of the $\Lambda_c(2880)^+$, *Phys. Rev. Lett.* **98**, 262001 (2007).